arXiv:1203.3283v1 [cond-mat.str-el] 15 Mar 2012

Strong multiferroicity and giant magnetoelectric effect in $(Insulator)/(LaMnO_3)_n/(SrMnO_3)_n/(Insulator)$ heterostructure

Sudhakar Yarlagadda[1,2], Peter B. Littlewood[3,4,5], Pinaki Majumdar[6], and Ravindra Pankaj[2]
[1] *CAMCS and* [2] *TCMP Div., Saha Institute of Nuclear Physics, Kolkata, India*
[3] *Cavendish Lab, Univ. of Cambridge, Cambridge, UK*
[4] *Argonne National Laboratory, Argonne IL 60439*
[5] *University of Chicago, James Franck Institute, Chicago IL 60637 and*
[6] *Harish-Chandra Research Institute, Allahabad, India*
(Dated: February 27, 2013)

We demonstrate that manganite heterostructures of the form $(Insulator)/(LaMnO_3)_n/(SrMnO_3)_n/(Insulator)$ show strong multiferroicity with magnetic ordering being induced by ferroelectric charge ordering. Ferroelectric polarization is produced by charges leaking from $LaMnO_3$ side to the $SrMnO_3$ side on account of the effective nearest-neighbor repulsion of electrons resulting from electron-phonon interaction. The origin of the ferromagnetism is due to double exchange when a particle virtually hops to its unoccupied neighboring site and back. Furthermore, we also demonstrate that a striking giant magnetoelectric effect occurs due to the strong coupling between the charge and spin orderings.

PACS numbers: 75.85.+t, 71.38.-k, 71.45.Lr, 71.38.Ht, 75.47.Lx, 75.10.-b

I. INTRODUCTION

Oxides such as manganites display a rich interplay of various orbital, charge, and spin orders when rare-earth dopants are added to the parent oxide. While significant progress has been made in characterizing the bulk doped materials, the heterostructures produced from two parent oxides is an area of active research[1]. Several novel phenomena, that have no counter part in the bulk samples, seem to emerge from the interface/heterostructure physics[2]. In fact, the challenge is to technologically exploit this new physics and develop new useful devices that can meet future challenges such as miniaturization, dissipationless operation/manipulation (such as read/write capability), energy storage, etc.

There has been a revival in multiferroic research partly due to improved technology, discovery of new compounds (such as $YMnO_3$, $TbMn_2O_5$), need for devices with strong magnetoelectric effect, etc[3]. Majority of the multiferroics studied are bulk materials where it is not yet clear why the magnetic and electric polarizations coexist poorly[4]. With the advent of improved molecular-beam-epitaxy technology one can now grow oxide heterostructures and explore the possibility of strong multiferroic phenomena as well as large interplay between ferroelectricity and magnetic polarization. There are numerous mechanisms for magnetoelectric effect reviews for which can be found in Refs. 5–7. At the interface of a magnetic oxide and a ferroelectric/dielectric oxide, magnetoelectric effect of electronic origin has been predicted by some researchers. Upon application of an external electric field, not only the magnitude of moments can be changed[8,9], but in some cases the very nature of magnetic ordering can be changed[10].

In this paper we predict a giant magnetoelectric effect, not at the interface, but away from it, in an oxide-oxide heterostructure (see Fig. 1). Our objective is to present a plausible/possible unnoticed multiferroic phenomenon in manganite heterostructures and point out the associated large/striking magnetoelectric effect. Jahn-Teller electron-phonon interaction is shown to be key to understanding both multiferroicity and magnetoelectric effect in our oxide heterostructure. Here, we exploit the fact that manganites have various competing phases that are close in energy and that by using an external perturbation (such as an electric or a magnetic field) the system can be induced to alter its phase. We show that there is a charge redistribution (with a net electric dipole moment perpendicular to the interface) and a concomitant ferromagnetism due to the optimization produced by the following two competing effects: (i) energy cost to produce holes on the $LaMnO_3$ (LMO) side and excess electrons on the $SrMnO_3$ (SMO) side; and (ii) energy gain due to electron-hole attraction (or electron-electron repulsion) on nearest-neighbor Mn-sites induced by electron-phonon interaction. The charge polarization is akin to that of a pn-junction in semiconductors although the governing equations are different. The key results of our analysis are: (i) the interface charge density at the LMO-SMO interface is 0.5 electrons/site and the charge in the layers perpendicular to the interface rapidly attain the bulk value as one moves away from the interface due to the fact that the dielectric constant is not large; (ii) the LMO-SMO interface is ferromagnetic and persists to be ferromagnetic for a few layers adjacent to the interface on both sides of the interface; (iii) furthermore, since ferroelectricity and ferromagnetism have a common origin [i.e., holes (electrons) on LMO (SMO) side], there is a striking interplay between these two polarizations leading to a giant magnetoelectric effect.

The rest of the paper is organized as follows. In Sec. II we introduce our phenomenological Hamiltonian (based on cooperative Jahn-Teller physics) using which we deduce the charge distribution in Sec. III and establish the ferroelectric effect of our oxide-oxide heterostructure. Next, in Sec. IV we show how the charge profile across the interface produces magnetic phases (much like the phase diagram of LSMO) and show how the interface charge affects magnetism on both sides of it. We close in Sec. V with our concluding observations.

II. POLARONIC HAMILTONIAN

In our $(Insulator)/(LaMnO_3)_n/(SrMnO_3)_n/(Insulator)$ heterostructure depicted in Fig. 1, we expect to realize the entire phase diagram of $La_{1-x}Sr_xMnO_3$ starting with the $x = 0$ phase at the Insulator-LMO interface and sequentially evolving to the $x = 1$ phase at the other end involving SMO-Insulator interface. Since, majority of the LSMO phase diagram (including the end regions near $x = 0$ and $x = 1$) is taken up by insulating phases, we expect that there is no effective transport in the direction normal to the oxide-oxide interface. Furthermore, we will show that the calculated concentrations in any layer on both the LMO and SMO sides turn out to be such that the bulk $La_{1-x}Sr_xMnO_3$ (LSMO) at this concentration is always in the insulating regime. Thus, we consider a system of localized electrons: This is also in tune with the insulating behavior reported in $(SrMnO_3)_n/(LaMnO_3)_{2n}$ superlattices[14–16]. Additionally, at strong electron-phonon coupling, one can see that band width is significantly diminished. Other reasons for localization, besides narrow band electrons being localized by disorder (such as interface roughness), could be anti-ferromagnetic order on the SMO side and cooperative lattice Jahn-Teller distortion on the LMO side. Then, *for analyzing the charge distribution normal to the interface*, the starting Hamiltonian is assumed to have the following phenomenological form:

$$H^{pol}_{eff} \sim -\left[\gamma^1_{\rm ep} g^2\omega_0 + \frac{\gamma^2_{\rm ep} t^2}{g^2\omega_0}\right] \sum_{j,\delta} n_j(1 - n_{j+\delta}), \quad (1)$$

where the first coefficient $\gamma^1_{\rm ep} g^2\omega_0$ is due to electron-phonon interaction and represents nearest-neighbor electron-electron repulsion brought about by incompatible distortions of nearest-neighbor oxygen cages surrounding occupied Mn ions. The pre-factor $\gamma^1_{\rm ep}$ can depend on the phase – for instance, in the C-type antiferromagnetic (AFM) regime of LSMO, $\gamma^1_{\rm ep}$ is expected to be large because occupancy of neighboring d_{z^2} orbitals is inhibited in the z-direction; while in the A-type AFM regime (corresponding to undoped $LaMnO_3$), $\gamma^1_{\rm ep}$ is expected to be weaker because of compatible Jahn-Teller distortions on neighboring sites. Here we will assume for simplicity that $\gamma^1_{\rm ep}$ is concentration independent and that $0.1 \le \gamma^1_{\rm ep} \le 1$. Next, the coefficient $\gamma^2_{\rm ep} t^2/(g^2\omega_0)$ results from processes involving hopping to nearest-neighbor and back and is present even when we consider the simpler Holstein model[11] or the Hubbard-Holstein model[12]. The pre-factor $\gamma^2_{\rm ep}$ varies between 1/2 (for non-cooperative electron-phonon interaction) and 1/4 (since for cooperative breathing mode in one-dimensional chains $\gamma^2_{\rm ep} = 1/3$, which should be more than in C-chains)[13]. Now, since manganites are two-band systems, $t^2/g^2\omega_0$ is an effective term which has contributions from hopping between various orbitals on neighboring sites and the polaronic energy associated with different orbital occupancy. Furthermore, although n_j is the total number in both orbitals on site j, it can only take a maximum value of 1 due to strong on-site electron-electron repulsion and strong Hund's coupling. Next, to make the above Hamiltonian furthermore relevant for manganites, one needs to consider Hund's coupling between core spins and itinerant electrons. This leads to invoking the double exchange mechanism for transport. Then, the hopping term t_{ij} between sites i and j in Eq. (1) is modified to be $t_{ij}\sqrt{0.5[1 + (\mathbf{S}_i \cdot \mathbf{S}_j/\mathbf{S}^2)]}$. Lastly, we ignored the effect of superexchange interaction in the starting effective Hamiltonian in Eq. (1) because its energy scale is significantly smaller that the polaronic energy term $g^2\omega_0$ and thus its effect on charge distribution can be neglected.

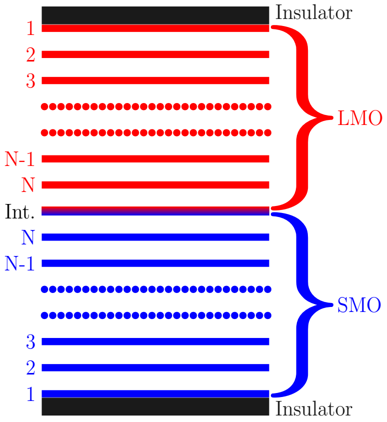

FIG. 1. (Color online) Schematic showing the $(Insulator)/(LaMnO_3)_N/(SrMnO_3)_N/(Insulator)$ heterostructure. Each of the labelled N layers on both LMO and SMO sides, as well as in the Interface, comprise of manganese-oxide (MO) layers.

III. CHARGE PROFILE

For a localized system, we only need to minimize the interaction energy which is a functional of the electronic density profile. The Coulombic interaction energy resulting from the electrons leaking from the LMO side to the SMO side, is taken into account by ascribing an effective charge +1 (hole) to the LMO unit cell (centered at the Mn site) that has donated an e_g electron from the Mn site and effective charge −1 (electron) to the SMO unit cell (centered at the Mn site) that has accepted an e_g electron at the Mn site. The Coulombic energy that results is due to interactions between these ±1 effective charges. The net positive charge on the LMO side and net negative charge on the SMO side will produce a charge polarization (or inversion asymmetry). Since the ferroelectric dipole is expected to be in the direction perpendicular to the oxide-oxide (LMO-SMO) interface, we assume that the density is uniform in each layer for calculating the density profile as a function of distance z from the insulator-oxide interface. The Coulombic interaction energy per unit area due to leaked charges is the same for both LMO and SMO regions and is given, in the continuum approximation, to be

$$E_{coul} = \frac{1}{8\pi\epsilon}\int_0^L dz D(z)^2, \tag{2}$$

where $D(z)$ is the electric displacement and is given by

$$D(z) = \pm\left[-\epsilon \mathrm{E}_{ext} + \int_0^z dy 4\pi e\rho(y)\right], \tag{3}$$

with $+$ $(-)$ sign for LMO (SMO) side. Furthermore, $\rho(z)$ is the charge density, e the charge of a hole, ϵ the dielectric constant, E_{ext} an external electric field along the z-direction, and L the thickness of the LMO (SMO) layers.

The ground state energy per unit area [corresponding to the effective Hamiltonian of Eq. (1)] can be written, in the continuum approximation, as a functional of $\rho(z)$ for both LMO and SMO as follows:

$$E_{pol} = -\left[\gamma^1_{\mathrm{ep}} g^2\omega_0 + \frac{\gamma^2_{\mathrm{ep}} t^2}{g^2\omega_0}\right]\zeta\int_0^L dz\rho(z)[1-a^3\rho(z)], \tag{4}$$

where $\zeta = 6$ is the coordination number and a is the lattice constant. In arriving at the above equation we have approximated $n_{i+\delta} + n_{i-\delta} \approx 2n_i$. Furthermore, for the ground state, we expect $t_{ij}\sqrt{0.5[1+(\mathbf{S}_i\cdot\mathbf{S}_j/\mathbf{S}^2)]} = t_{ij}$, i.e., minority charges completely polarize the neighboring majority charges.

We will now minimize the total energy given below

$$E_{Total} = 2E_{pol} + 2E_{coul}, \tag{5}$$

by setting the functional derivative $\delta E_{Total}/\delta\rho(z)$ =0. This leads to the following equation

$$0 = -C_1[1-2a^3\rho(z)] + 2C_2\int_z^L dy\left[-\tilde{\mathrm{E}}_{ext} + \int_0^y dx\rho(x)\right], \tag{6}$$

where $C_1 \equiv \left[\gamma^1_{\mathrm{ep}} g^2\omega_0 + \frac{\gamma^2_{\mathrm{ep}} t^2}{g^2\omega_0}\right]\zeta$; $C_2 \equiv 2\pi e^2/\epsilon$; and $\tilde{\mathrm{E}}_{ext} \equiv \epsilon\mathrm{E}_{ext}/(4\pi e)$. The above equation, upon taking double derivative with respect to z, yields

$$C_1 a^3\frac{d^2\rho(z)}{dz^2} - C_2\rho(z) = 0. \tag{7}$$

The above second-order differential Eq. (7) and Eq. (6) admit the solution

$$\rho(z) = \frac{1}{2a^3}\frac{\cosh(mz)}{\cosh(mL)} + m\tilde{\mathrm{E}}_{ext}\frac{\sinh[m(L-z)]}{\cosh(mL)}, \tag{8}$$

where $m = \sqrt{C_2/(C_1a^3)}$. It is important to note that for the manganese-oxide (MO) layer at the LMO-SMO interface (i.e., at $z = L$), the density is 0.5 electrons/site and that it is independent of the applied external electric field! Furthermore, for realistic values of the parameters, the charge density rapidly changes as we move away from the oxide-oxide interface (i.e., after only a few layers from the interface) and attains values close to the bulk value. Lastly, as required for zero values of field E_{ext}, we get $\rho(0) \to 0$ when $L \to \infty$. Thus, although we used the continuum approximation, our obtained density profile is qualitatively realistic as it has the desired values at the extremes $z = L$ and $z = 0$ with the density away from the LMO-SMO interface rapidly falling for not too large values of ϵ.

For our calculations we used the following values for the parameters: $a = 4$ Å; $\epsilon = 20$; 0.05 eV $\leq \omega_0 \leq$ 0.07 eV; $2 \leq g \leq 3$; and 0.2 eV $\leq t \leq$ 0.6 eV. The density profiles for both LMO and SMO sides depend only on ϵ, C_1 and E_{ext}. We observe from Figs. 2 and 3 that for smaller values of C_1, as distance from the interface increases, the density falls more rapidly while the density change due to electric field rises faster.

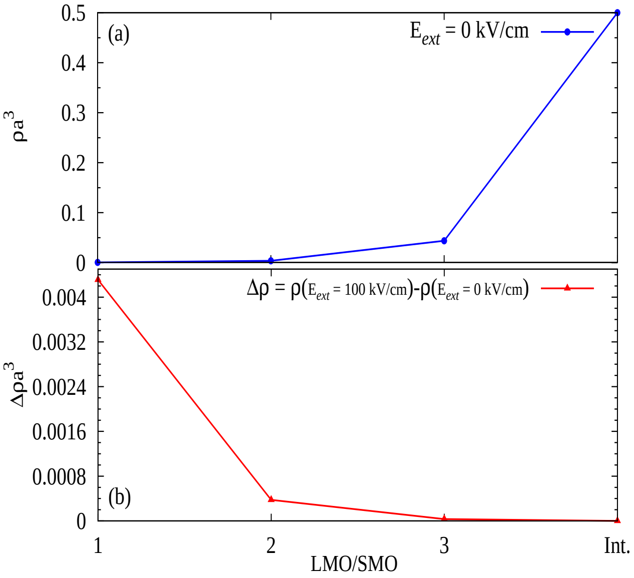

FIG. 2. (Color online) Minority-charge density ρ in various layers (on both LMO and SMO sides) of a $(Insulator)/(LaMnO_3)_3/(SrMnO_3)_3/(Insulator)$ heterostructure for $a = 4$ Å, $\epsilon = 20$, and $C_1 = 0.19$. Displayed results are for (a) ρ at $\mathrm{E}_{ext} = 0$ kV/cm and (b) $\Delta\rho = \rho(\mathrm{E}_{ext} = 100\text{ kV/cm}) - \rho(\mathrm{E}_{ext} = 0\text{ kV/cm})$. This system does not show a significant magnetoelectric effect due to low density ρ away from the interface.

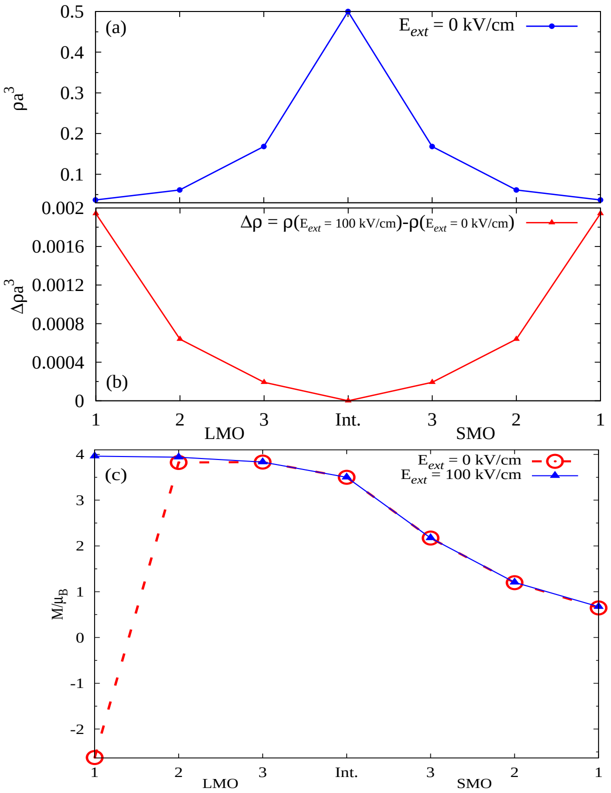

FIG. 3. (Color online) Minority-charge density ρ and magnetization M/μ_B in various manganese-oxide layers (on both LMO and SMO sides) of a $(Insulator)/(LaMnO_3)_3/(SrMnO_3)_3/(Insulator)$ heterostructure for a = 4 Å, ϵ = 20, and C_1 = 0.93. Depicted figures are for (a) $\rho(\mathrm{E}_{ext}$ = 0 kV/cm); (b) $\Delta\rho = \rho(\mathrm{E}_{ext}$ = 100 kV/cm$) - \rho(\mathrm{E}_{ext}$ = 0 kV/cm); and (c) M/μ_B at E_{ext} = 0 kV/cm and E_{ext} = 100 kV/cm. Manganese-oxide (MO) layer 1 on the LMO side undergoes spin reversal when an external field E_{ext} is applied.

IV. MAGNETIZATION DISTRIBUTION

We will now obtain the magnetization for a heterostructure by considering its lattice structure unlike the case for the density profile where a continuum approximation was made. Thus we can take into account the possibility of antiferromagnetic order besides being able to consider ferromagnetic order.

First, we observe that the bulk $La_{1-x}Sr_xMnO_3$ (below the magnetic transition temperatures) is A-type antiferromagnetic (AFM) for $0 \leq x \lesssim 0.1$; ferromagnetic insulator (FMI) for $0.1 \lesssim x \lesssim 0.15$; and ferromagnetic (FM) metal for $0.15 \lesssim x \lesssim 0.5$[17]. Hence, we model the LMO side of the heterostructure as a ferromagnet in regions with hole concentrations that are large but less than 0.5 with the magnetic structure abruptly switching to an A-type AFM as the hole concentration values decrease to about 0.1 or less. Next, we note that for $0.5 \lesssim x \lesssim 1.0$, the LSMO bulk system is always an AFM insulator with A-type AFM for $0.5 \lesssim x \lesssim 0.65$; C-type AFM for $0.65 \lesssim x \lesssim 0.95$; and G-type AFM for $0.95 \lesssim x \lesssim 1.0$. Thus, from a magnetism point-of-view, the magnetic moment on the SMO side of the heterostructure is expected to be zero except in the vicinity of the interface where (due to proximity effect) it will be FM and can be modeled using a percolating picture. Given the above scenario, as can be expected, we find that the FM region on the LMO side can be drastically enhanced (at the expense of the A-type AFM region) by an electric field inducing holes on the LMO side. On the hand, the electric field has only a small effect on the percolating FM cluster that is adjacent to the oxide-oxide interface and is on the SMO side.

A. SMO side

We will first consider the SMO side and show that the magnetization decays as we move away from the LMO-SMO interface. We derive the largest FM domain as follows. On account of nearest-neighbor repulsion (as given in Eq. (1)), the interface (which is half-filled) has e_g electrons on alternate sites. In fact, to minimize the inter-

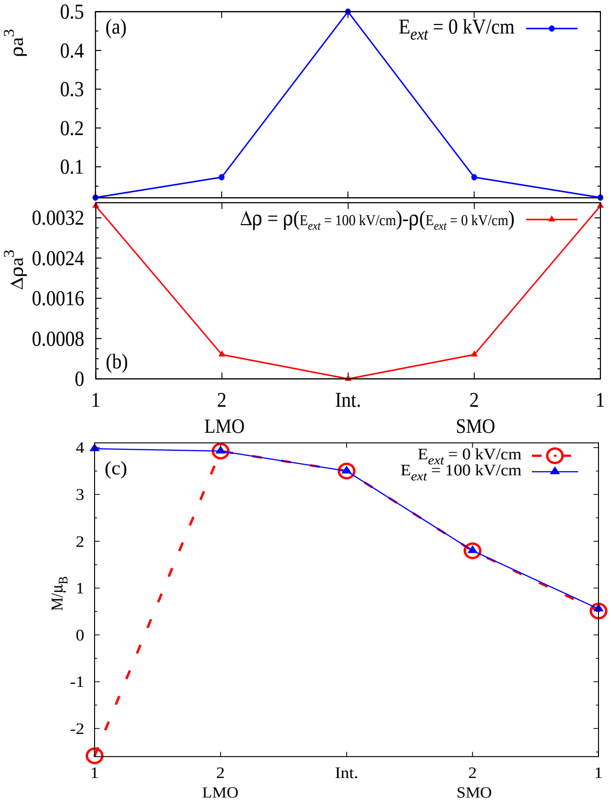

FIG. 4. (Color online) Minority-charge density ρ and magnetization M/μ_B in various manganese-oxide layers of a $(Insulator)/(LaMnO_3)_2/(SrMnO_3)_2/(Insulator)$ heterostructure for $a = 4$ Å, $\epsilon = 20$, and $C_1 = 0.30$. Figures are for (a) $\rho(\mathrm{E}_{ext} = 0$ kV/cm); (b) $\Delta\rho = \rho(\mathrm{E}_{ext} = 100$ kV/cm$) - \rho(\mathrm{E}_{ext} = 0$ kV/cm); and (c) M/μ_B at $\mathrm{E}_{ext} = 0$ kV/cm and $\mathrm{E}_{ext} = 100$ kV/cm. MO layer 1 on the LMO side undergoes spin reversal when E_{ext} is applied.

action energy, on the SMO side we take the e_g electrons to be in one sub-lattice only (i.e., they are in the same sub-lattice in each layer but on alternate sub-lattices on adjacent layers). On account of virtual hopping, an e_g electron polarizes all its neighboring sites that do not contain any e_g electrons. Thus we observe that the half-filled interface will be fully polarized and that there will be a FM cluster that begins at the interface and percolates to the layers away from the interface on the SMO side. For instance, in the layer next to the oxide-oxide interface, all the e_g electrons are next to sites unoccupied by e_g electrons at the interface and hence are FM aligned with the interface; similarly, again in the adjacent layer, all the sites in the sub-lattice unoccupied by e_g electrons have the same polarization as the sites occupied by e_g electrons at the interface. The probability that a site, occupied (unoccupied) by an e_g electron, contributes to the FM cluster is equal to the probability of finding the site occupied (unoccupied) multiplied by 1-P where P is the probability of not having any of the adjacent sites unoccupied (occupied) and belonging to the percolating cluster. Thus, we obtain the following set of coupled equations:

$$x_N^{e_g} = \rho(z_N)[1-(1-2x_{N-1}^u)(1-2x_N^u)^4(1-2x_{N+1}^u)], \quad (9)$$

$$x_N^u = 0.5[1-(1-2x_{N-1}^{e_g})(1-2x_N^{e_g})^4(1-2x_{N+1}^{e_g})], \quad (10)$$

where $x_N^{e_g}$ (x_N^u) is the concentration of polarized sites that belong to the spanning cluster and these sites are a subset of the sites in the sub-lattice occupied (unoccupied) by e_g electrons in the N^{th} two-dimensional (2D) MO layer with N being the index measured from the Insulator-SMO interface. Furthermore, z_N is the z-coordinate of the N^{th} 2D MO layer. The factor $(1-2x_N^{e_g})$ $[(1-2x_N^u)]$ represents the probability of a site that belongs to the sub-lattice occupied (unoccupied) by e_g electrons in layer N but is not part of the spanning polarized cluster. The boundary conditions involving layer 1 are

$$x_1^{e_g} = \rho(z_1)[1-(1-2x_1^u)^4(1-2x_2^u)], \quad (11)$$

$$x_1^u = 0.5[1-(1-2x_1^{e_g})^4(1-2x_2^{e_g})], \quad (12)$$

while those for the LMO-SMO interface are $x_{\text{Int}}^{e_g} = x_{\text{Int}}^u = 0.5$.

B. LMO side

Next, we will show that a few-layered LMO side can be border-line ferromagnetic [i.e., it is either barely fully ferromagnetic or close to being fully ferromagnetic] which can be exploited to obtain giant magneto-electric effect. Similar to the bulk situation[18], in our heterostructure as well, we assume that in each MO layer two e_g electrons on adjacent sites have the same ferromagnetic coupling $J_{xy} = 1.67$ meV while two e_g electrons on adjacent layers have again the same antiferromagnetic coupling $J_z = 1.2$ meV. On the other hand, for an electron and a hole on adjacent sites in the same MO layer or adjacent MO layers, (due to virtual hopping of electron between the two sites) there is a strong ferromagnetic coupling $J_{eh} = t^2/(2g^2\omega_0) >> J_{xy}$[19]. In our calculations, as long as the ratio of J_{xy}/J_z is fixed and J_{eh} is the significantly dominant coupling, we get the same magnetic picture.

When only a few MO layers are present in LMO, we will show that an LMO side that is not fully FM can be dramatically switched to being fully FM (by increasing the concentration of holes in the layers) upon application of a large external field. To establish this, we assume that the LMO-SMO interface and all MO layers up to M are completely polarized. Next, we assume that MO layers M and $M-1$ have low density of holes so that there is a possibility that spins in MO layer $M-1$ are not aligned with all MO layers up to layer M. We then analyze (in Appendix A) the polarization of MO layer $M-1$ by comparing the energies for the following two cases:

(i) layers $M-1$ and M are antiferromagnetically aligned with the holes in layers M and $M-1$ inducing polarization only on sites that are adjacent to the holes; and

(ii) MO layer $M-1$ is completely polarized and aligned with Layer M.

In an LMO system that is three unit cell thick, for $C_1 = 0.93$ eV (as shown in Fig. 2), we obtained a striking magneto-electric effect. For zero external field, when $M = 2$ is considered, case (i) has lower energy, i.e., layer 1 is antiferromagnetically coupled to layer 2. On the other hand, when a strong electric field (~ 100 kV/cm) is applied, MO layer 1 (due to increased density of holes) becomes completely polarized and ferromagnetically aligned with the rest of the layers (i.e., MO layers 2, 3, and the oxide-oxide interface). *Thus, we get a giant magneto-electric effect!* Similarly, in a $(Insulator)/(LaMnO_3)_2/(SrMnO_3)_2/(Insulator)$ heterostructure, for $C_1 = 0.30$ eV (as shown in Fig. 3), we again obtain a huge magneto-electric effect.

V. CONCLUSIONS

We used the fact that when the two Mott insulators LMO and SMO are brought together to form a heterostructure, one may realize the entire phase diagram of $La_{1-x}Sr_xMnO_3$ across the heterostructure with the $x = 0$ phase occurring at the LMO surface at one end and evolving to the $x = 0.5$ state at the oxide-oxide interface and finally to the $x = 1$ phase at the other end of SMO.

By changing the charge profile using an applied electric field, we showed that the FMI region can be expanded at the expense of the A-type AFM domain thereby producing a giant magnetoelectric effect. Since the competing phases at the interface of the FMI and the A-type AFM region are close in energy, the interface can be tuned to be on the verge of a FM transition by the application of a magnetic field of the order of a Tesla (as the Zeeman energy is comparable to the difference in the FM coupling J_{xy} and the AFM coupling J_z); then, applying a tiny electric field will produce a FM transition at the interface.

We also would like to mention that if a superlattice were formed from the heterostructure $(Insulator)/(LaMnO_3)_n/(SrMnO_3)_n/(Insulator)$, then the dipoles from each repeating heterostructure unit will add up to produce a giant electric dipole moment. On the other hand, if the insulating layers were not present, the superlattice formed from the repeating unit $(LaMnO_3)_n/(SrMnO_3)_m$ would not produce a large electric dipole as the charge from LMO can leak to SMO on both sides leading to a small net dipole moment.

Lastly, minimizing the energy expressed as a functional of density and magnetization at a fixed electric field (so as to get simultaneously both charge and magnetization profiles) is more accurate (albeit tedious) than solving, as we did, for the charge profile and using it to get the magnetization picture. This better alternative can also address the issue of how an external magnetic field affects the density profile and the ferroelectric moment.

Appendix A

In this appendix, we will analyze the nature of magnetism on the LMO side. To begin, we assume that all MO layers from M to the oxide-oxide interface (i.e., MO layers M, $M+1$, ...) are completely polarized. We then bring a completely polarized MO layer to form the layer $M-1$ next to the MO layer M and wish to determine the interaction energy between layer $M-1$ and layer M and their relative polarization. We compare the energies in the following two scenarios:

(i) MO layer $M-1$ is antiferromagnetically aligned with layer M and there is an induced polarization next to the holes in these layers, i.e., all the sites that are adjacent to the holes in layers M and $M-1$ end up having the same polarization as the holes; and

(ii) MO layer $M-1$ is completely polarized and ferromagnetically aligned with Layer M.

The energy of interaction in case (i) is the sum of the two terms T_a and T_b obtained below:

(a) when an electron in the electron sub-lattice of layer M is not surrounded by a hole in either layer M or layer $M+1$ [the probability of which is $(1-2\rho(z_M))^4\,(1-2\rho(z_{M+1}))$], then the hole in layer $M-1$ flips the spin of the electron below it in layer M. Contrastingly, a hole in layer M will always flip the spin of the electron above it in layer $M-1$. The resultant electron-hole interaction energy is $-J_{eh}\times[\rho(z_M)+\rho(z_{M-1})]$. The flipping of spins by holes changes the interaction between the spins and their four neighbors in the xy-plane and yields the interaction energy $2\times J_{xy}\times[\rho(z_{M-1})\times 4+\rho(z_M)\times 4]$. Furthermore, there is an additional antiferromagnetic coupling between layer M and $M-1$ which is given by $-J_z\times[1-\rho(z_M)]$ where the antiferromagnetic coupling between layers is reduced due to holes in layer M. Thus the resultant interaction energy is

$$\begin{aligned} T_a = &\left[(1-2\rho(z_M))^4\,(1-2\rho(z_{M+1}))\right] \\ &\times[-J_{eh}\times[\rho(z_M)+\rho(z_{M-1})] \\ &\quad+2J_{xy}\times[4\rho(z_{M-1})+4\rho(z_M)] \\ &\quad-J_z\times[1-\rho(z_M)]]\,. \end{aligned} \tag{A1}$$

(b) When an electron in the electron sub-lattice of layer M is surrounded by at least one hole in either layer M or layer $M+1$ [the probability of which is $1-(1-2\rho(z_M))^4\,(1-2\rho(z_{M+1}))$], then the hole in layer $M-1$ and its 4 neighbors in the same layer flip their spins to align with the spin of the electron below the hole in layer $M-1$. On the other hand, a hole in layer M always flips the spin of the electron above it in layer $M-1$. The resultant electron-hole interaction energy is $-J_{eh}\times[\rho(z_M)+\rho(z_{M-1})]$. The flipping of spins changes the interaction between the flipped spins and their neighbors in the plane and yields the interaction energy $2\times J_{xy}\times[\rho(z_{M-1})\times 4\times 3+\rho(z_M)\times 4]$. Additionally, there is a new antiferromagnetic coupling between layer M and $M-1$ given by $-J_z\times[1-\rho(z_M)-\rho(z_{M-1})\times(1+4\times 2)]$ where the antiferromagnetic coupling between layers is reduced due to holes in layers M and $M-1$ and flipped electron spins in layer $M-1$. Thus the resultant interaction energy is

$$\begin{aligned} T_b = &\left[1-(1-2\rho(z_M))^4\,(1-2\rho(z_{M+1}))\right] \\ &\times[-J_{eh}\times[\rho(z_M)+\rho(z_{M-1})] \\ &\quad+2J_{xy}\times[12\rho(z_{M-1})+4\rho(z_M)] \\ &\quad-J_z\times[1-\rho(z_M)-9\rho(z_{M-1})]]\,. \end{aligned} \tag{A2}$$

Next, the interaction energy for case (ii) is given by sum of the following two terms T_c and T_d:

(c) $T_c=-J_{eh}\times[\rho(z_M)+\rho(z_{M-1})]$; and

(d) $T_d=J_z\times[1-\rho(z_M)-\rho(z_{M-1})]$.

---

[1] C. H. Ahn, A. Bhattacharya, M. Di Ventra, J. N. Eckstein, C. Daniel Frisbie, M. E. Gershenson, A. M. Goldman, I. H. Inoue, J. Mannhart, Andrew J. Millis, Alberto F. Morpurgo, Douglas Natelson, and Jean-Marc Triscone, Rev. Mod. Phys. **78**, 1185 (2006).

[2] One striking example is the interface of $LaAlO_3/SrTiO_3$ system reported in A. Ohtomo and H. Hwang, Nature **427**, 423 (2004); N. C. Bristowe, Emilio Artacho, P. B. Littlewood, Phys. Rev. B **80**, 045425 (2009); N. C. Bristowe, P. B. Littlewood, Emilio Artacho, J. Phys.: Condens. Matter **23**, 081001 (2011).

[3] For a review see J. P. Velev, S. S. Jaswal and E. Y. Tsymbal, Phil. Trans. R. Soc. A **369**, 3069 (2011).

[4] D.I. Khomskii, J. Magn. Magn. Mater, **306**, 1 (2006).

[5] D. Khomskii, Phys. **2**, 20 (2009).

[6] K. F. Wang, J. M. Liu, and Z. F. Ren, Adv. Phys. **58**, 321 (2009).

[7] M. Fiebig and N. A. Spaldin, Eur. Phys. J. B **71**, 293 (2009).

[8] J. M. Rondinelli, M. Stengel,and N. A. Spaldin, Nat. Nanotechnol. **3**, 46 (2008).

[9] M. K. Niranjan, J. D. Burton, J. P. Velev, S. S. Jaswal, and E. Y. Tsymbal, Appl. Phys. Lett. **95**, 052501 (2009).

[10] J. D. Burton and E. Y. Tsymbal, Phys. Rev. B **80**, 174406 (2009).

[11] S. Datta, A. Das, and S. Yarlagadda, Phys. Rev. B **71**, 235118 (2005).

[12] S. Reja, S. Yarlagadda, and P. B. Littlewood, Phys. Rev. B **84**, 085127 (2011).

[13] S. Yarlagadda, e-print arXiv:0712.0366v2; Ravindra Pankaj and Sudhakar Yarlagadda (to be published).

[14] A. Bhattacharya, S. J. May, S. G. E. te Velthuis, M. Warusawithana, X. Zhai, Bin Jiang, J.-M. Zuo, M. R. Fitzsimmons, S. D. Bader, and J. N. Eckstein, Phys. Rev. Lett. **100**, 257203 (2008).

[15] S. Smadici, P. Abbamonte, A. Bhattacharya, X. Zhai, B. Jiang, A. Rusydi, J. N. Eckstein, S. D. Bader, and Jian-Min Zuo, Phys. Rev. Lett. **99**, 196404 (2007).

[16] C. Adamo, X. Ke, P. Schiffer, A. Soukiassian, M. Warusawithana, L. Maritato, and D. G. Schlom Appl. Phys. Lett. **92**, 112508 (2008).

[17] A. Szewczyk, M. Gutowska and B. Dabrowski, Phys. Rev. B **72**, 224429 (2005).

[18] N. N. Kovaleva, Andrzej M. Oleś, A. M. Balbashov, A. Maljuk, D. N. Argyriou, G. Khaliullin, and B. Keimer, Phys. Rev. B **81**, 235130 (2010).

[19] For an explanation of the ferromagnetic-insulator region of LSMO see G. V. Pai, S. R. Hassan, H. R. Krishnamurthy, and T. V. Ramakrishnan, Europhys. Lett. **64**, 696 (2003).